Distribution Agreement

In presenting this thesis or dissertation as a partial fulfillment of the requirements for an advanced degree from Emory University, I hereby grant to Emory University and its agents the non-exclusive license to archive, make accessible, and display my thesis or dissertation in whole or in part in all forms of media, now or hereafter known, including display on the world wide web. I understand that I may select some access restrictions as part of the online submission of this thesis or dissertation. I retain all ownership rights to the copyright of the thesis or dissertation. I also retain the right to use in future works (such as articles or books) all or part of this thesis or dissertation.

Signature:

_____ _____

Rui Liu Date

Creation of Tubular α–Helical Assemblies Through Seven-Helix Coiled Coils

By

Rui Liu

Master of Science

Chemistry

_____
Vincent P. Conticello
Advisor

_____
Elliott L. Chaikof
Committee Member

_____
David Lynn
Committee Member

Accepted:

_____
Lisa A. Tedesco, Ph.D. Dean of the James T. Laney School of Graduate Studies

_____
Date

Creation of Tubular α–Helical Assemblies Through Seven-Helix Coiled Coils

By

Rui Liu

B.S. Peking University, 2008

Advisor: Vincent P. Conticello, Ph.D.

An abstract of

A thesis submitted to the Faculty of the

James T. Laney School of Graduate Studies of Emory University

in partial fulfillment of the requirements for the degree of

Master of Science

in Chemsitry

2010

Abstract

Creation of Tubular α–Helical Assemblies Through Seven-Helix Coiled Coils

By Rui Liu

Native coiled-coil sequences can form large bundles composed of four or more helices in which the helix packing arrangements define continuous channels throughout the supramolecular structure. If the number of helices within the assembly and the inter-helical packing arrangements could be controlled, then one might be able to tailor the channel dimensions and chemistry to facilitate binding of specific classes of guest molecules. A recently reported example of a coiled-coil channel based on a seven-helix bundle provides a prototype for the design of such channels from simple helical peptides. The investigators expanded the hydrophobic interface between helices, which resulted in a discrete seven-helix bundle that defined a channel with an interior diameter of 7 Å. A single residue shift in helix registry was observed between adjacent helices, which resulted in an overall shift of seven residues upon closure of the bundle structure. The structure of the seven-helix bundle resembles a screw with an axial translation corresponding to seven residues within the helical assembly. By modifying the sequence of the peptide to promote end-to-end association between the ends of the lock washer structure, peptide **7HSAP1a** was created which could self-associate into a helical fibril, and peptide **7HSAP1a-Cap** was created as a negative control. CD spectropolarimetry was used to confirm the helical structure of the peptides. TEM studies indicate the presence of high aspect-ratio fibrils of uniform diameter of 7.4 nm for the **7HSAP1a** in MES buffer (pH 6.0). The self-assembly behavior for **7HSAP1a** peptide was enhanced in MES buffer (pH 6.0, 100 mM KF), but was weakened in distilled H_2O. In the case of capped peptide **7HSAP1a-Cap**, self-assembly of fibrils was greatly inhibited after thermal annealing of peptide solutions. Fluorescence spectroscopy confirmed the anticipation that the **7HSAP1a** peptide might form coiled-coil channel which trapped PRODAN.

Creation of Tubular α–Helical Assemblies Through Seven-Helix Coiled Coils

By

Rui Liu

B.S. Peking University, 2008

Advisor: Vincent P. Conticello, Ph.D.

A thesis submitted to the Faculty of the

James T. Laney School of Graduate Studies of Emory University

in partial fulfillment of the requirements for the degree of

Master of Science

in Chemsitry

2010

Acknowledgments

I would like to thank my advisor, Dr. Vincent P. Conticello for his instruction and support for my research and thesis preparation. I appreciate the opportunity to work with him, which has provided me with valuable experience and knowledge.

I also want to thank my committee members Dr. Elliott L. Chaikof and Dr. David Lynn for their guidance in my research.

I want to express my sincere thanks to my lab members Melissa Patterson, Weilin Peng, I-lin Wu, Yunyun Pei and Chunfu Xu for their help in my work.

I also would like to thank all the faculty and staff of the Department of Chemistry for their generous help.

Table of Contents

List of Figures

Figure 13.CD spectropolarimetry of peptide **7HSAP1a** (12.57 μM in 10 mM MES buffer pH 6.0) before (blue) and after (red) thermolysis at 95 °C and extended annealing at 25 °C

Figure 14.CD spectropolarimetry of peptide **7HSAP1a** (50.29 μM in 10 mM MES buffer pH 6.0 with 100 mM KF) before (blue) and after (red) thermolysis at 95 °C and extended annealing at 25 °C

Figure 15.CD spectropolarimetry of peptide **7HSAP1a** (49.61 μM in H_2O) before (blue) and after (red) thermolysis at 95 °C and extended annealing at 25 °C

Figure 16.CD spectropolarimetry of peptide **7HSAP1a-CAP** (68.34 μM in 10 mM MES buffer pH 6.0) before (blue) and after (red) thermolysis at 95 °C and extended annealing at 25 °C

Figure 17.CD spectropolarimetry of peptide **7HSAP1a-CAP** (68.34 μM in 10 mM MES buffer pH 6.0 with 100mM KF) before (blue) and after (red) thermolysis at 95 °C and extended annealing at 25 °C

Figure 18.TEM image of high aspect-ratio fibrils that result from self-assembly of peptide **7HSAP1a** (50.29 μM in 10 mM MES buffer pH 6.0) thermolysis at 95 °C and extended annealing at 25 °C (scale bar = 100 nm)

Figure 19.TEM image of high aspect-ratio fibrils that result from self-assembly of peptide **7HSAP1a** (50.29 μM in 10 mM MES buffer pH 6.0) thermolysis at 95 °C and extended annealing at 25 °C (scale bar = 200nm)

Figure 20.TEM image of high aspect-ratio fibrils that result from self-assembly of peptide **7HSAP1a** (12.57 μM in 10 mM MES buffer pH 6.0) thermolysis at 95 °C and extended annealing at 25 °C (scale bar = 200nm).

Figure 21.TEM image of peptide **7HSAP1a-CAP** (68.34 μM in 10 mM MES buffer pH 6.0) thermolysis at 95 °C and extended annealing at 25 °C (scale bar = 500nm).

Figure 22.TEM image of peptide **7HSAP1a** (50.29 μM in 10 mM MES buffer pH 6.0 with 100mM KF) thermolysis at 95 °C and extended annealing at 25 °C (scale bar = 200nm)

Figure 23.TEM image of peptide **7HSAP1a** (49.61 μM in H_2O) thermolysis at 95 °C and extended annealing at 25 °C (scale bar = 500nm)

Figure 24.Fluorescence spectra for 588.44 μM PRODAN in DMF and 2.57 μM PRODAN in 10 mM MES buffer (pH 6.0)

Figure 25. Fluorescence spectra for 2.57 μM PRODAN in **7HSAP1a-CAP** peptide solutions in 10 mM MES buffer (pH 6.0) at different concentrations with or without thermal annealing at 95 °C

Figure 26. Fluorescence spectra for 2.57 μM PRODAN in 250 μM **7HSAP1a** peptide solutions in 10 mM MES buffer (pH 6.0) at temperature range from 25 °C to 75 °C

Figure 27. Fluorescence spectra for 2.57 μM PRODAN in 250 μM **7HSAP1a-Cap** peptide solutions in 10 mM MES buffer (pH 6.0) at temperature range from 25 °C to 75 °C

Creation of Tubular α–Helical Assemblies Through Seven-Helix Coiled Coils

Introduction:

Development of Peptide-Based Biomaterials:

The study of peptide-based biomaterials is of great interest as it helps us understand how natural biomaterials are constructed and suggests promising applications in biotechnology and synthetic biology [1]. The most promising approach towards fabrication of molecular biomaterials is through the production of supramolecular architectures via self-assembly of structural sub-units. The critical issue that must be addressed in the rational design of the molecules that are competent for self-assembly is the selection of sequence to favor the target structure and disfavor structurally similar alternatives.

The most common structural motifs for the design of peptide-based materials are β-strands and α–helices (Figure 1). β-structured systems, which form structurally defined fibrils through intermolecular hydrogen bond interactions, have been dominated the peptide biomaterials field, as the sequences tend to be short and are easily accessible through conventional solid-phase peptide synthesis [1]. However, recently, more and more attention has begun to focus on the study of α–helical-based systems due to a greater potential for controlling peptide self-assembly through de novo design [1]. α-helical coiled-coil peptides are promising candidates for the creation of functional supramolecular materials through applications of *de novo*

design principles, in which structure may be modified to respond to changes in the environment.

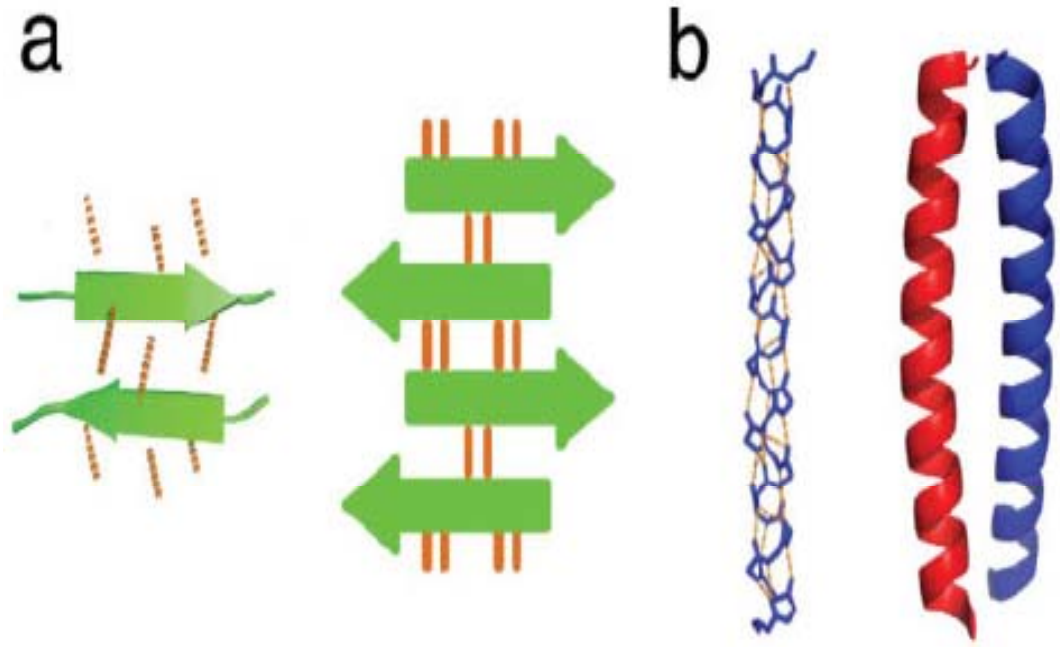

Figure 1. Basic (a) β-strand and β-sheet, (b) α–helical and coiled-coil [1]

α-Helical Coiled-Coil Peptides

The coiled-coil is a common structural motif in proteins [2]. Native coiled-coil sequences can form large bundles composed of four or more helices. Their supercoiled structures are encoded by seven-residue repeats denoted as $[\boldsymbol{abcdefg}]_n$ (Figure 2). Within a helix, 3.6 residues form a complete turn; thus a heptad corresponds to approximately two turns of the helix [3]. Typically, ***a***- and ***d***- positions are nonpolar core residues at the interface of the two helices, which form the supercoiled α-helical structures through a "knob-into-holes" packing pattern [4]. In addition, the ***e***- and ***g***- positions are usually occupied by charged, polar residues,

which are connected through electrostatic interactions between the two helices, and contribute to the stability of the coiled-coil [4].

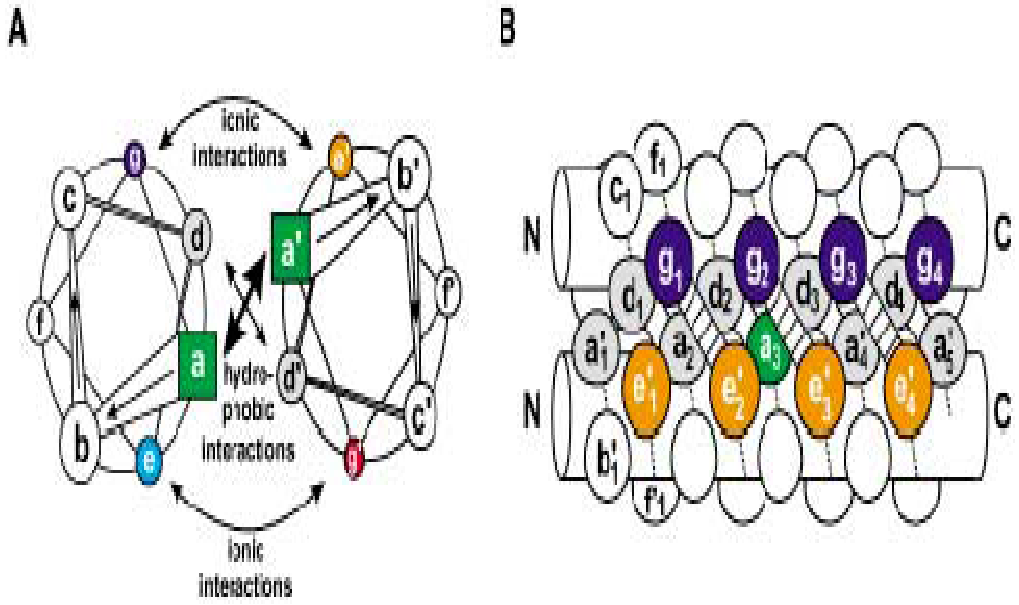

Figure 2. Schematic representation of a parallel, dimeric coiled coil [3]. A provides a helical wheel diagram and B provides a side view. Residues are labeled ***a-g*** in one helix and ***a***'-***g***' in another helix.

Tremendous insight into coiled-coil structure has been gained from the examination of sequence-variants of the leucine zipper domain of the *S. cerevisiae* protein GCN4, a transcriptional activator for amino acid biosynthesis [5]. The wild-type GCN4 leucine zipper, which contains leucine residues at the ***d***- position in a heptad repeat, is a two-stranded parallel coiled coil. By altering the hydrophobic/polar patterning of the coiled-coil heptad, a variety of structures have been created. The GCN4 mutants have been designed by changing the ***a***-, ***d***-, ***e***-, ***f***- residues on or around the interface between the two helices, to investigate their effects on coiled-coil folding and assembly [6]. A large number of structural variants, including dimers, trimers, tetramers, and pentamers have been reported, which vary in their helix orientation and alignment [7]. Small changes in hydrophobicity at ***a***- and ***d***- positions change the oligomerization state of the GCN4 derivatives, which can be rationalized in terms of the packing of the hydrophobic side-chains at the helix-helix interfaces. Changing ***a***- and/or ***d***- residues to non-natural amino acids with higher hydrophobic character can also influence the oligomerization state and thermodynamic stability of the coiled-coil structure [8]. The changes induced through amino acid substitutions at the hydrophobic interface can be quite subtle, for example, mutation of an asparagine residue located at a core ***a***- position to a valine changed the peptides forming a trimer instead of a dimer [9]. In addition, a parallel five-helix coiled-coil could be converted to a four-helix coiled-coil through substitution of a single Phe residue to Met within a core Phe hydrophobic interface (Figure 3) [10].

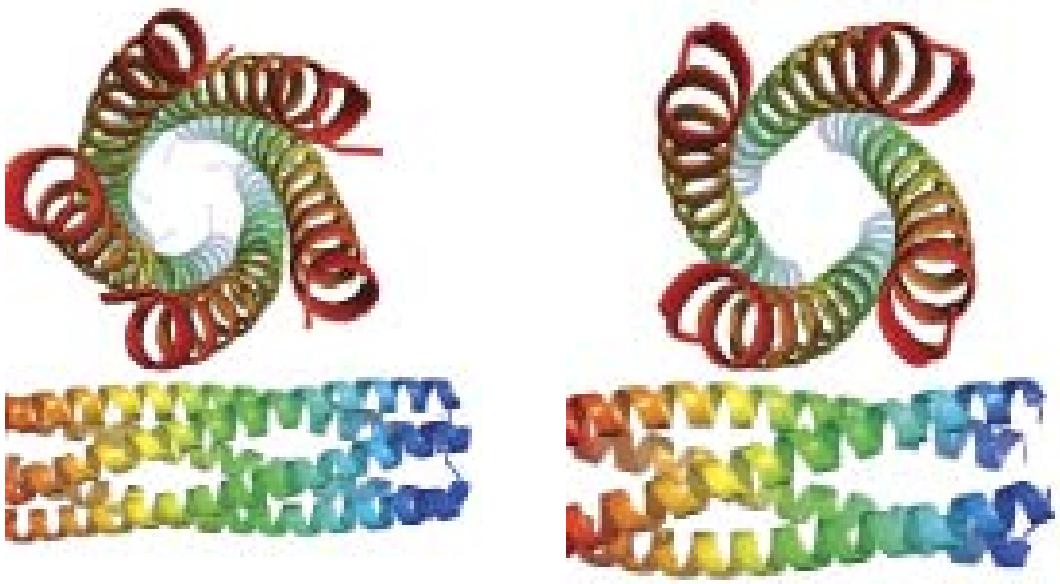

Figure 3. Left: A coiled-coil with phenylalanine at all ***a***- and ***d***- positions folds as a parallel pentamer. Right: a tetramer is formed if one of the phenylalanines is substituted by methionine [10].

The nature of the electrostatic ***e***- and ***g***- residues, which are commonly glutamic acid and lysine, can strongly influence the pairing specificity. The ***g***/***e***' residues play an important role in determining homo- versus heterotypic paring, parallel versus antiparallel orientation, and the oligomerization states of the helical chains in coiled-coils [11]. For example, Hu's group changed the oligomerization state of the GCN4 by altering ***g***/***e***' residues [12]. They constructed a pool of more than 65,000 GCN4 leucine zipper mutants with different combinations of alanine, glutamic acid, lysine, or threonine at the ***e***- and ***g***- positions, in which about 90 % mutants did not form stable homooligomers, less than 3 % formed stable homodimers, and 8 % had phenotypes consistent with the formation of higher-order oligomers [12].

The Seven-Helix Coiled Coil

In the superamolecular structure formed by the α-helical coiled-coil peptides, the helix-helix packing arrangements define continuous channels. If the number of helices within the assembly and the inter-helical packing arrangements could be controlled, then one might be able to tailor the channel dimensions and chemistry to facilitate binding of specific classes of guest molecules. Although the *de novo* design of such structures has been postulated, thus far the only examples have been observed have resulted from structural characterization of a single native α-helical cylinders [13]. However, a recently reported example of a coiled-coil channel based on a seven-helix bundle provides a prototype for the design of such channels from simple helical peptides [14].

Lu's group investigated a GCN4 leucine zipper variant containing exclusively alanine residues at the ***e***- and ***g***- positions (Figure 4), which formed a stable helical heptamer in aqueous solution [14]. By expanding the hydrophobic interface between helices, the peptide resulted in a discrete seven-helix bundle that defined a channel with an interior diameter of 7 Å (Figure 5) [14]. Moreover, a single residue shift in helix registry was observed between adjacent helices, which resulted in an overall shift of seven residues (i.e., one coiled-coil heptad repeat) upon closure of the bundle structure. In contrast, most coiled-coil structures have no corresponding shift in helix registry and result in discrete bundles, while the seven-helix bundle resembles a screw (or lock washer) with an axial translation corresponding to seven residues within the helical assembly.

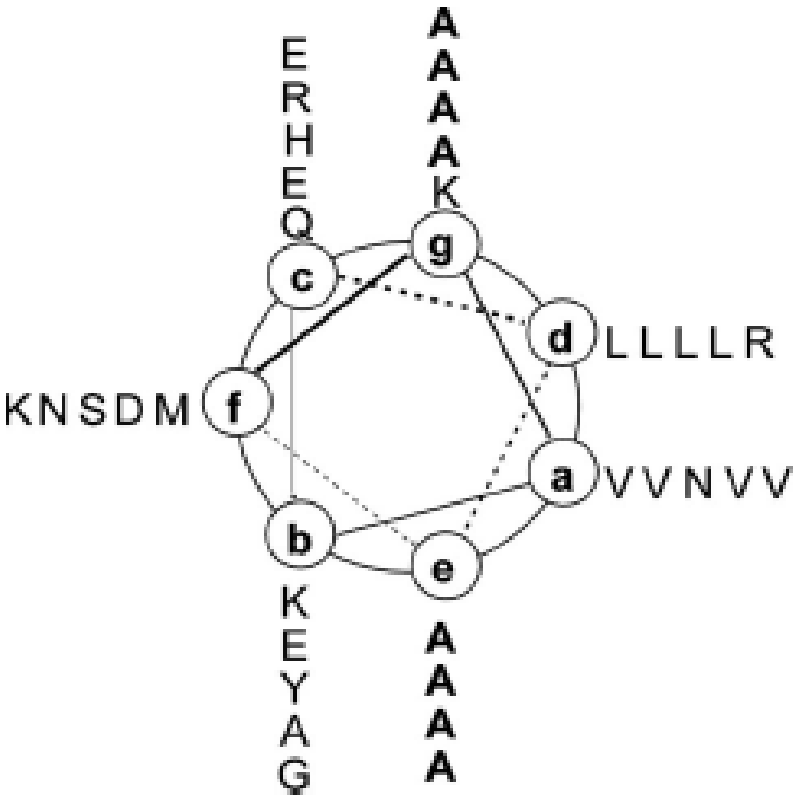

Figure 4. Helical wheel projection of residues Met-1 to Arg-34 of the GCN4-pAA sequence. The view is from the *N*-terminus. GCN4-pAA differs from most conventional coiled-coil structures by substitution of alanine at four ***e***- and ***g***- positions (bold) [14].

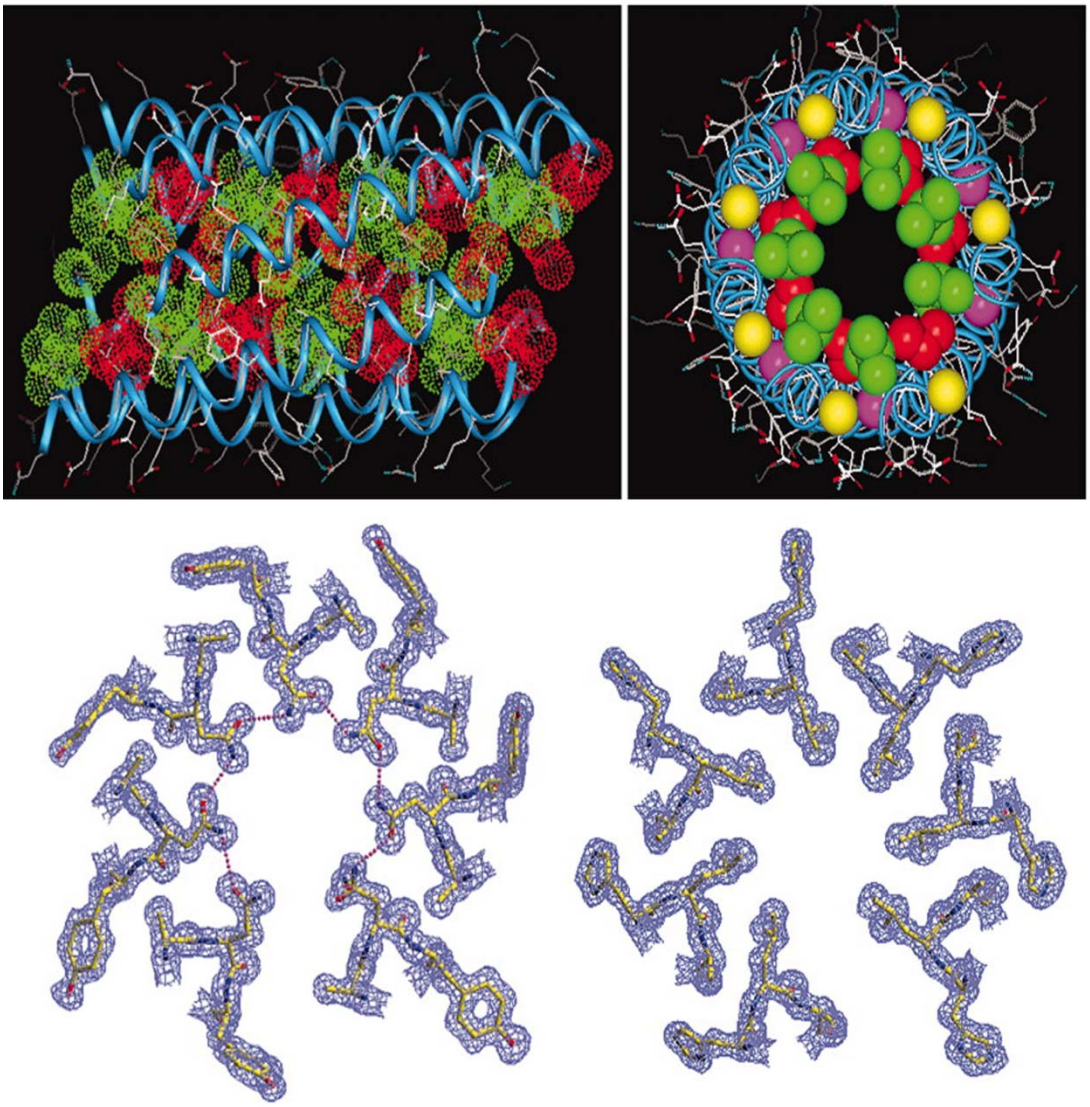

Figure 5. Top: Crystal structure of a seven-helix, coiled-coil assembly resulting from self-association of a GCN4-p1 peptide with an expanded hydrophobic interface, indicating full-length and top-down views (left and right, respectively). Bottom: Cross-sectional views of the packing of residues at the helical interface in a selected ***a***-layer (left) and ***d***-layer (right), in which the right-handed helical screw symmetry can be observed [14].

Therefore, if the sequence of the peptide was appropriately modified to promote end-to-end association between the ends of the lock washer structure, then the structure would self-associate into a helical fibril with a continuous channel corresponding in dimensions to the crystal structure of the original peptide. The peptide, **7HSAP1a** (Figure 6), was designed and prepared via solid-phase peptide synthesis. The hydrophobic interface of the original peptide was maintained as we reasoned that this feature was necessary to ensure formation of the seven-helix bundle. However, the electrostatic interactions were maximized between the spatially proximal ***b***- and ***c***- positions on adjacent helices (Figure 6). In addition, a net charge of (+2) was placed on each peptide to hinder lateral association between bundles. The *N*- and *C*-termini of the peptide were left uncapped in order to promote electrostatic attraction between the lock washer structures at the interface between the ends of the helices. As a control, a capped peptide of identical sequence was prepared in anticipation that capping would hinder self-association.

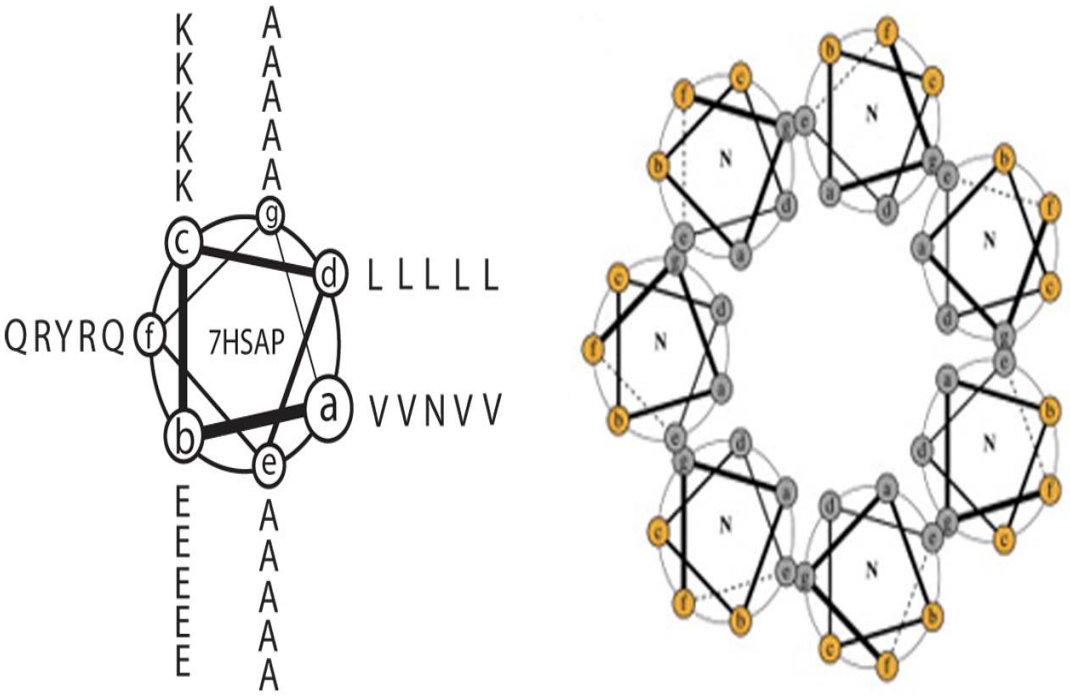

Figure 6. Left: Amino acid sequence of **7HSAP1a** projected onto a helical wheel in supercoil space. The expanded hydrophobic interface consists of amino acid residues at the ***a***-, ***d***-, ***e***-, and ***g***-positions within the heptad repeat sequence. Right: Top view of the packing arrangement of helices within a layer of the seven-helix bundle of **7HSAP1a**.

Experimental Methods

Materials

All chemical reagents and suppliers were purchased from Fisher Scientific (Pittsburgh, PA) or Sigma Chemical Corporation (St. Louis, MO) unless otherwise specified. The 200 mesh carbon-coated copper grids, uranyl acetate (UA), and phosphotungstic acid (PTA) used as stain for Transmission Electron Microscopy were purchased from Electron Microscopy Science (Washington, PA). The 1.00 mm sealed quartz cell used for Circular Dichroism spectroscopy was purchased from Hellma (USA). The 10 mm fluorometer cell used for Fluorescence Study was purchased from Starna Cells (Atascadero, CA).

Design of the Peptides

Based on the successful synthesis of the first seven-helix heptamer (Figure 4), the peptide **7HSAP1a** (Figure 6) was designed having the amino acid sequence below.

KLAQAVEKLARAVEKLAYANEKLARAVEKLAQAVE

Several critical structural features were considered when modifying the sequence. The hydrophobic interface, i.e. ***a***-, ***d***-, ***e***-, and ***g***- positions, was maintained from the sequence of GCN4-pAA, as it was deemed essential to the formation of the seven-helix bundle. However, by replacing all the amino acids at ***b***-position with glutamic acid and ***c***-position with lysine, the electrostatic interactions were

maximized between the adjacent helices. In addition, a net charge of (+2) was introduced on each peptide to hinder lateral association between bundles. The *N*- and *C*-termini of the peptide were left uncapped in order to promote electrostatic attraction between the lock washer structures at the interface between the ends of the helices. As a control, a peptide of identical sequence, **7HSAP1a-CAP**, was prepared in which the *N*-terminus was capped with an acetyl group and the *C*-terminus with an amide. We anticipated that capping of the peptide would hinder end-to-end association, and, therefore, could be used to evaluate arrested intermediates on the self-assembly pathway.

Synthesis of the Peptides

The peptides were synthesized through the solid-phase peptide synthesis, either at GenScript (Piscataway, NJ) or in-house on a CEM Liberty microwave synthesizer. The **7HSAP1a** peptide has a molecular weight (MW) of 3823.46 and a purity of 90.7 %. The **7HSAP1a-CAP** peptide has a molecular weight of 3864.58 and a purity of 95.1 %. The peptides were obtained as white lyophilized powders and were stored at -20 °C

Solid-phase peptide synthesis (SPPS) is now the accepted method for synthesizing peptides and proteins in the lab (Figure 7). It allows the synthesis of peptides that are difficult to express in biological systems, as well as the incorporation of unnatural amino acids and amino acids with side-chain modifications. SPPS experiences a

process of coupling-wash-deprotection-wash. The free *N*-terminal amine of a solid-phase attached peptide is coupled to a single *N*-protected amino acid unit, which is deprotected, exposing a new *N*-terminal amine for further amino acid coupling steps. Wash cycles are performed after each reaction, removing excess reagent from a growing peptide that is covalently attached to an insoluble resin.

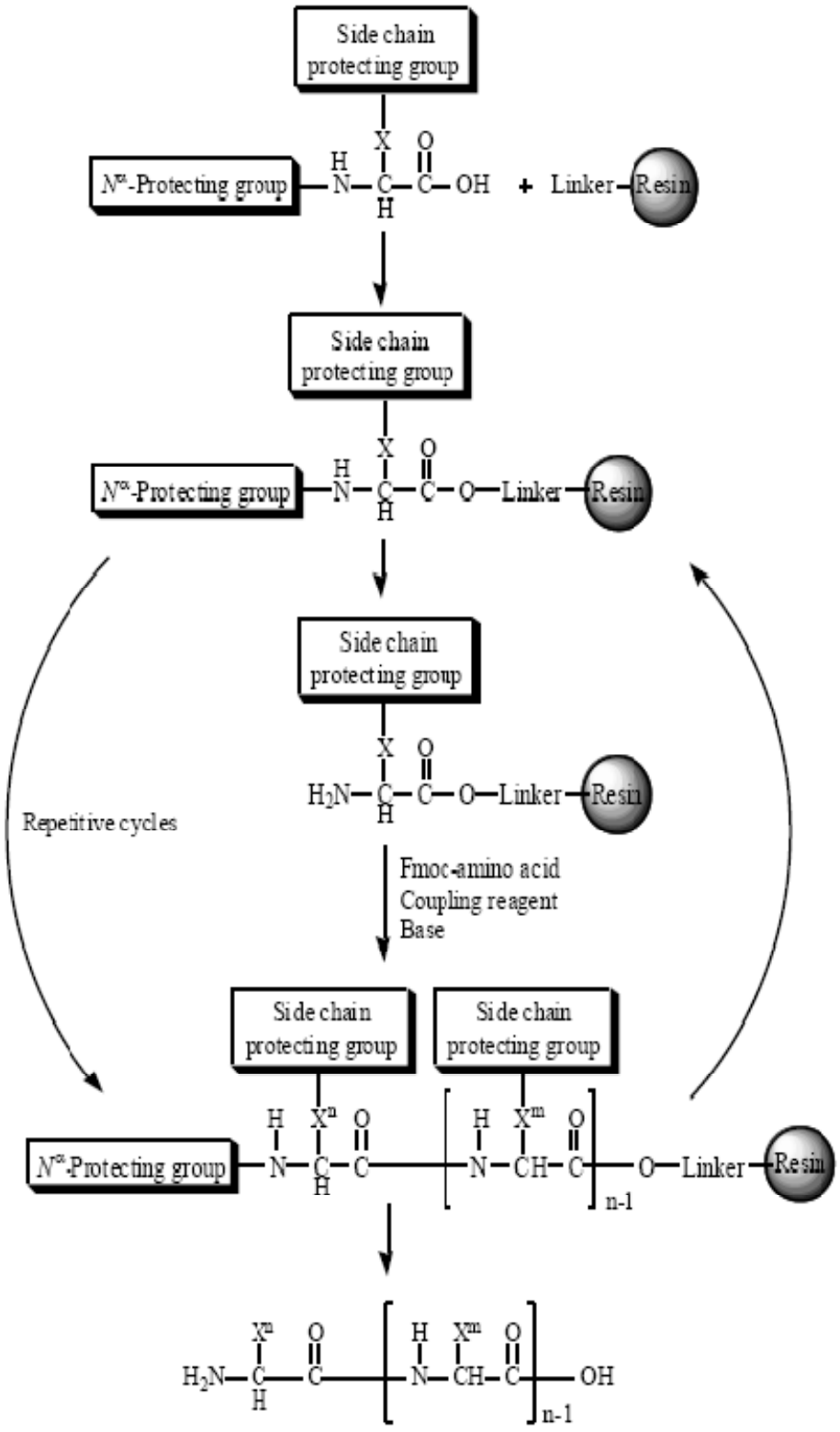

Figure 7. General steps for SPSS [15].

The two schemes of N-terminal protection used in SPSS are *tert*-(butoxy) carbonyl (Boc) group and the (9*H*-fluoren-9-ylmethoxy) carbonyl (Fmoc) group, which both proceed in a C-terminal to N-terminal direction. The *N*-termini of the amino acid monomer is protected by the two groups and added onto a deprotected amino acid chain. The original proposed strategy is the Boc chemistry, where Boc is removed by weak acids, usually 25 – 50 % trifluoroacetic acid (TFA) in dichloromethane (DCM), and stronger acid such as hydrogen fluoride (HF) or trifluoromethanesulfonic acid (TFMSA) was used in the final cleavage of the peptide [15]. However, the repetitive treatment of TFA might influence the yield for a long sequence in the Boc synthesis. Therefore, alternative method was developed. Fmoc protecting group proposed by Louis Carpino [16] is a base-labile group, which could be removed by a basic reagent, usually 20 % piperidine in DMF, and the final cleavage can be obtained with TFA [16]. The Fmoc chemistry soon proved to be cleaner, reliable and suitable for automation, which has great advantage of synthesizing long peptides. With the technical improvements at the end of the 1990s and beginning of the 2000s, microwave synthesizers have been designed to assist peptide synthesis, which enable the temperature of the reaction mixture could be controlled [17]. Microwave irradiation has been used to complete long peptide sequences with high degrees of yield and low degrees of racemization. The peptide synthesized in-house was obtained using Liberty automated peptide synthesizer through standard Fmoc chemistry.

Determination of the Peptide Concentration

The **7HSAP1a** and **7HSAP1a-CAP** peptides were dissolved in 10 uM MES buffer (pH 6.0) or in distilled H_2O. The peptide concentration was determined spectrophotometrically by measuring the absorbance at 280 nm (A_{280}) using an Ultrospec 3000 UV/Visible Spectrophotometer (Pharmacia Biotech, England). The concentration of peptides containing Tyr, Trp or Cys residues could be calculated by the equation:

$$MW * A_{280} / c\ [mg/mL] = 1280\ n_y + 5690\ n_w + 120\ n_c$$

The n_y, n_w and n_c represent numbers of tyrosine, tryptophan and cysteine, respectively, in the peptide sequence. As the peptides **7HSAP1a** and **7HSAP1a-CAP** contain only one tyrosine residue per molecule, then

$$c\ [mg/mL] = MW * A_{280} / 1280$$

To eliminate errors in determination of absorbance that might occur as a result of UV light scattering caused by peptide self-assembly, samples were mixed with 6 M guanidinium chloride with a volume-radio of 1:9 and briefly heated to 100 °C in sealed tubes to completely denature the sample prior to performing the absorbance measurements.

Circular Dichroism

Circular Dichroism (CD) spectropolarimetry is a critical tool to investigate the secondary structure of peptides in solution. The CD signature for α-helices is distinctive with characteristic minima at 208 nm and 222 nm. CD spectra were recorded on a Jasco J-810 CD spectropolarimeter (Jasco Inc, Easton, MD) equipped with a PFD-425S Peltier temperature control unit in a 1.00 mm sealed quartz cell at a concentration of 12.57 μM **7HSAP1a** and 68.36 μM **7HSAP1a-CAP** in 10 mM MES buffer (pH 6.0)，50.29 uM **7HSAP1a** and 68.36 μM **7HSAP1a-CAP** in 10 mM MES buffer (100 mM KF, pH 6.0), and 49.61 uM **7HSAP1a** in H_2O . Spectra were recorded as an average of 10 scans from 260 nm to 190 nm at 25 °C with a scanning rate of 50 nm/min and with a resolution of 0.5 nm. For the thermal denaturation study, the temperature was increased by 1 °C/min from 25 °C to 95 °C with an equilibration time of 1 min prior to acquisition of each CD trace. CD spectra were obtained before and after the thermal denaturation. Spectra were baseline corrected before converting to mean residue ellipticities (MRE) using the conversion formula below:

$$[\Theta] = \Theta_{obs} * MW / (10 * l * c * n)$$

in which $\mathbf{\Theta_{obs}}$ is the observed ellipticity measured in millidegrees, **MW** is molecular weight of the peptide, **l** is the path length of the cell in centimeter, **c** is the peptide concentration in mg/mL, and **n** is the number of amino acids in the peptide sequence.

Transmission Electron Microscopy

Transmission Electron Microscopy (TEM) was used to investigate the morphology of aggregates that result from self-assembly. TEM is a microscopy technique, where a beam of electrons transmitted through an ultra thin specimen, interacted with it and then formed an image. The image is magnified and focused onto an imaging device to be detected by a sensor. TEM is capable of obtaining images of high resolution; thus has wide application in determination of structure and morphology in self-assembled materials.

Samples of peptides of 50.29 μM **7HSAP1a** and 68.36 μM **7HSAP1a-CAP** in 10 mM MES buffer (pH 6.0)，50.29 uM **7HSAP1a** and 68.36 μM **7HSAP1a-CAP** in 10 mM MES buffer (100 mM KF, pH 6.0), and 49.61 uM **7HSAP1a** in distilled H_2O were annealed at 95 °C for 5 min and gradually cooled to 25 °C with extended annealing overnight. Uranyl acetate (2 %) and phosphotungstic acid (2 %) solutions were prepared in distilled water and were used to stain the peptide specimens. Peptide samples (5 μL) were deposited onto 200 mesh carbon-coated copper grids for 1 min incubation period and excess liquid was wicked away. Specimens were then stained using uranyl acetate (2 %) or phosphotungstic acid (2 %) solution for 40 sec, and soaked off using a filter paper. Specimens were dried overnight in desiccator. TEM images were obtained on Hitachi 7500 instrument at 75 kV accelerating voltage.

Fluorescence Spectroscopy

Fluorescence spectroscopy was used to investigate the formation of channel by the peptides. 2.27mg N, N-Dimethyl-6-propionyl-2-naphthylamine (PRODAN) was added into 10mL DMF (spectroscopic gradient) to make the standard solution of fluorescent dye. The dye concentration was determined spectrophotometrically by measuring the absorbance at 360 nm (A_{360}) using an Ultrospec 3000 UV/Visible Spectrophotometer based Beer's Law as below:

$$Abs = \varepsilon * c * l$$

in which **l** is the length of the cell of 1 cm, **ε** equals to 18,000 $M^{-1}cm^{-1}$. The standard solution was covered by aluminum foil as the dye was light-sensitive. A final concentration of 2.57 uM PRODAN was added into 500 uL peptide solutions in MES buffer (pH 6.0).

Solvent polarity has a dramatic effect on the emission spectrum of PRODAN. The emission maximum shifts 150 nm between solutions of cyclohexane and water (Figure 8) [18]. The environment-sensitive nature of PRODAN thus could be used to investigate the formation of hydrophobic cavity of the peptides.

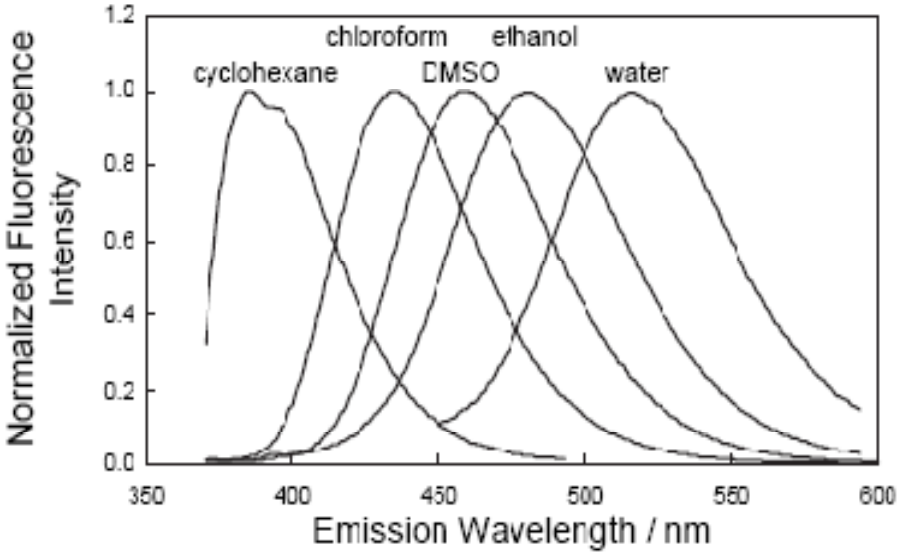

Figure 8. Normalized fluorescence emission spectra of 1uM PRODAN in different solutions (λex = 360 nm).

The fluorescence spectroscopy was studied on FluoroMax Spectrofluorometer (HORIBA, USA) equipped with MicroMax 384 microwell-plate reader. The excitation wavelength was set at 371 nm and the emission spectrum was obtained in wavelength range from 400 to 650 nm. The emission spectrum was recorded at room temperature and in temperature range from 25 ℃ to 75 ℃ increased by every 10 ℃ with an equilibration of 10 min at each temperature.

Results and Discussion

Synthesis of the Peptides:

The peptides **7HSAP1a** and **7HSAP1a-CAP** were purchased from GenScript (Piscataway, NJ). The purity of the peptides was analyzed by HPLC and the molecular weight of the peptides was confirmed by Electrospray Ionization Mass Spectrometry.

The purity of the **7HSAP1a** peptide is 90.7 % analyzed by GenScript using analytical HPLC on Alltima TM C18 column (4.6 * 250 mm). The peptide was eluded using a linear gradient at 1mL/min with solvent A consisting of water in 0.065 % trifluoroacetic acid (TFA), and solvent B consisting of acetonitrile in 0.05 % TFA. The gradient conditions were 5 % – 65 % solvent B for 25 min, 65 % – 95 % solvent B for 1 min, and then 95 % solvent B for 5 min (Figure 9). The column effluent was monitored at 220 nm in room temperature.

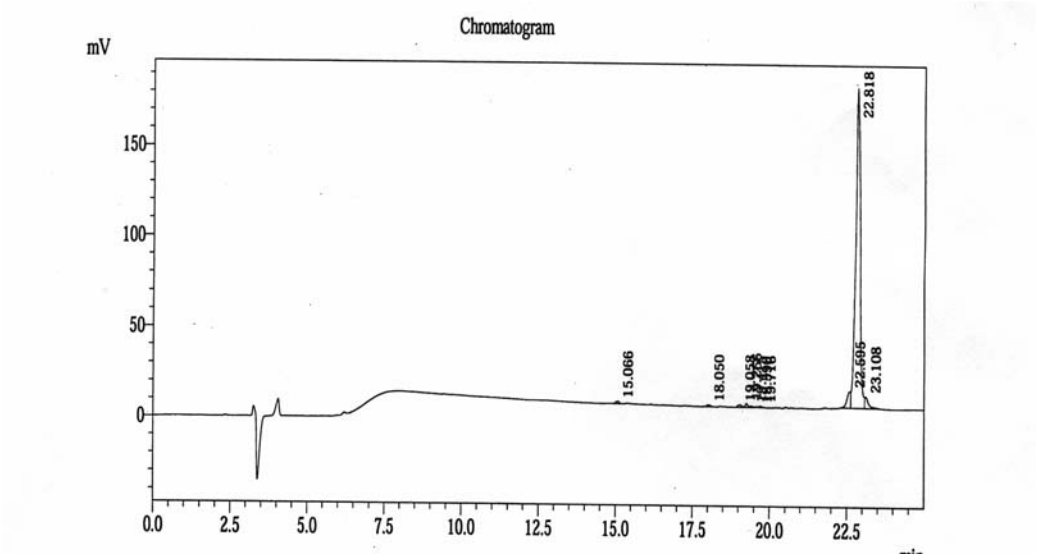

Figure 9. HPLC trace for **7HSAP1a.**

The purity of the **7HSAP1a-CAP** peptide is 95.1 % analyzed by GenScript using reversed phase HPLC on VYDAC C18 column (4.6 * 250 mm). The peptide was eluded using a linear gradient at 1mL/min with solvent A consisting of water in 0.1 % TFA, and solvent B consisting of acetonitrile in 0.1 % TFA. The gradient conditions were 35 % – 65 % solvent B for 25 min, 65 % – 100 % solvent B for 1 min, and then 100 % solvent B for 5 min (Figure 10). The column effluent was monitored at 220 nm in room temperature.

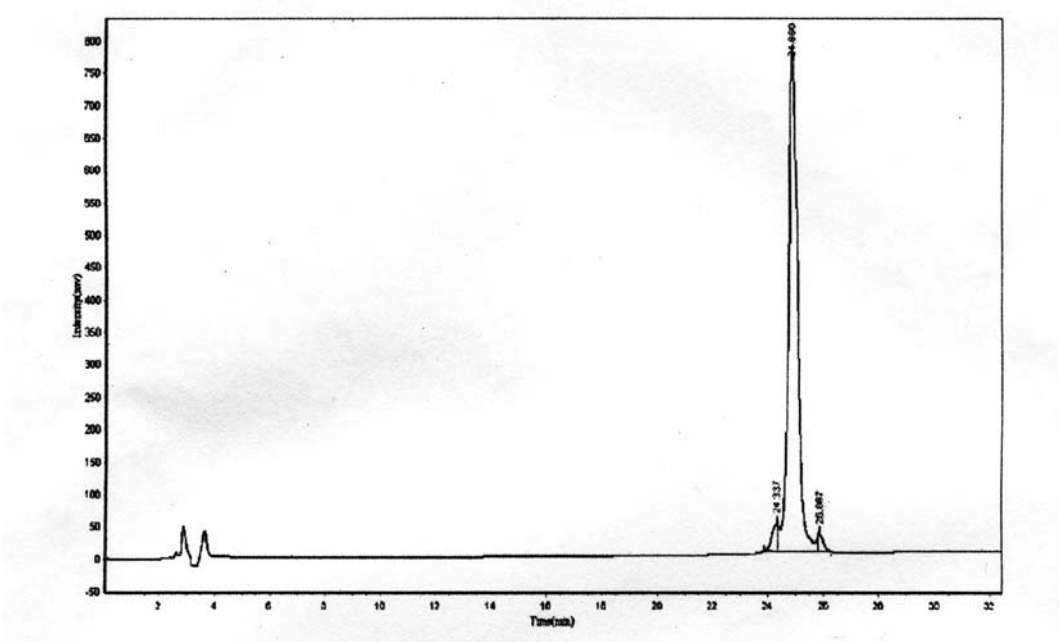

Figure 10. HPLC trace for **7HSAP1a.**

Electrospray Ionization Mass Spectrometry (ESI-MS) is used to investigate the structures of macromolecules, which is currently a powerful tool as it overcomes the propensity of these molecules to fragment when ionized. The mass spectra from ESI-MS analysis confirmed the identity of the **7HSAP1a** and **7HSAP1a-CAP** peptides (Figure 11 and Figure 12).

7HSAP1a ：

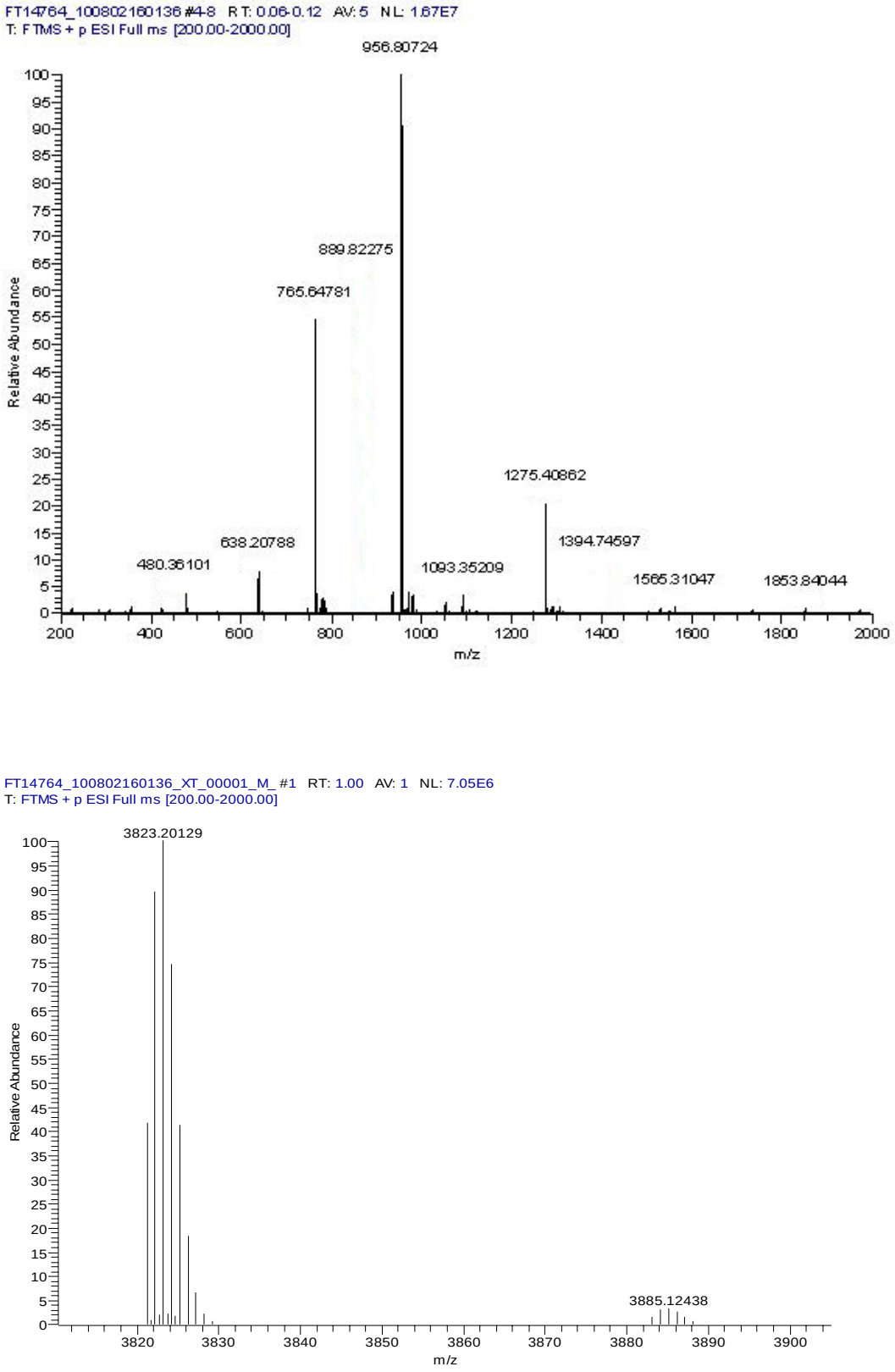

Figure 11. Mass spectrum for **7HSAP1a** (top) and its deconvolution (bottom).

7HSAP1a-CAP :

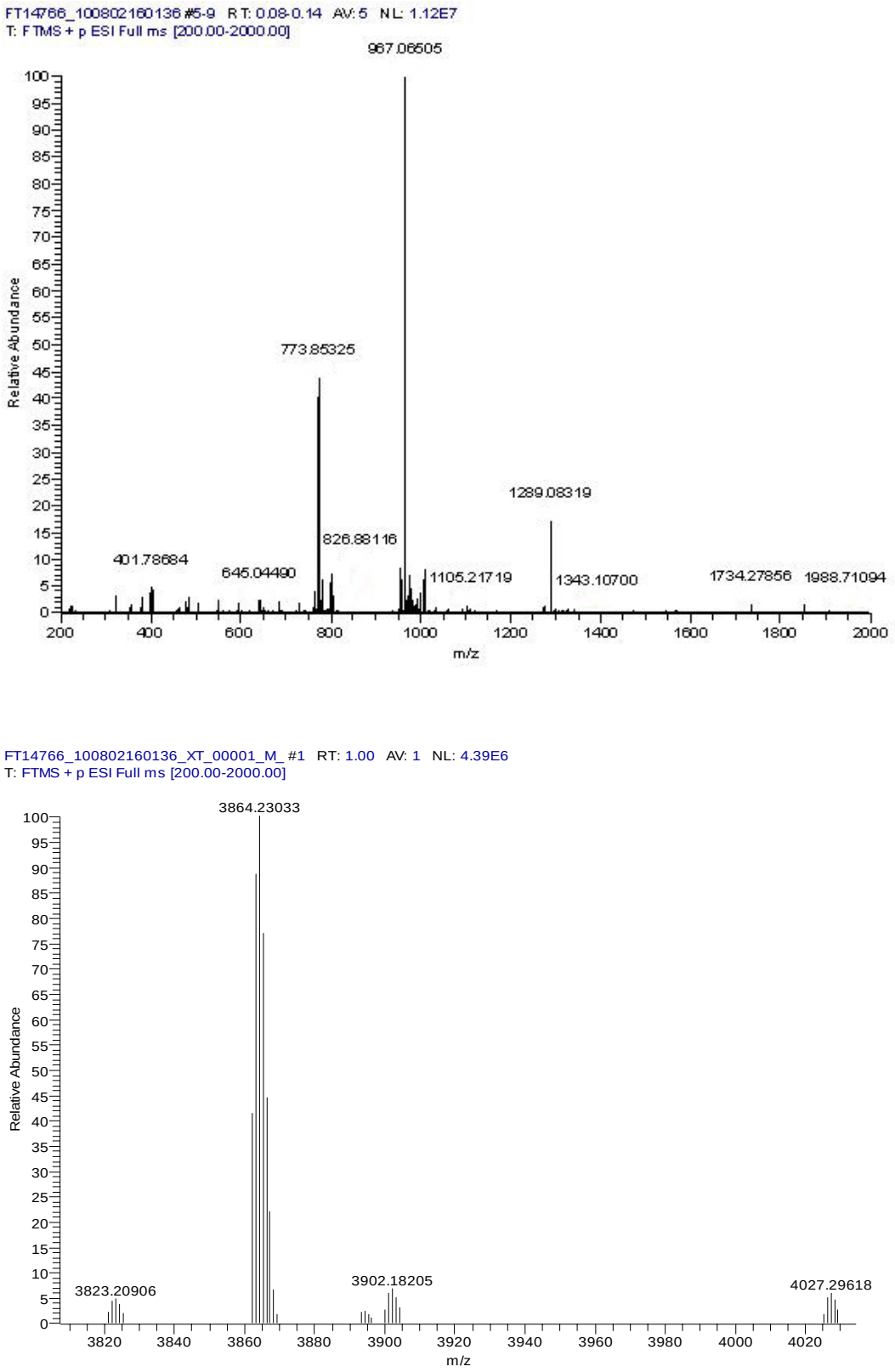

Figure 12. Mass spectrum for **7HSAP1a-CAP** (top) and its deconvolution (bottom).

Circular Dichroism

CD spectropolarimetry of peptide **7HSAP1a** indicated the presence of a helical conformation (Figure 13) with distinctive minima at 208 and 222 nm. However, the CD signal is strongly attenuated at shorter wavelengths due to scattering of the incident light, which becomes more pronounced after thermal annealing of the peptide specimen in 10 mM MES buffer (pH 6.0). CD signals are much weaker for **7HSAP1a** peptide in 10 mM MES buffer (100 mM KF, pH 6.0) before and after annealing (Figure 14), compared with the relative signals in 10 mM MES buffer (pH 6.0). However, CD signals before and after annealing remain the same for **7HSAP1a** peptide in distilled H_2O (Figure 15), which represents different behavior than was observed for the same peptide in MES buffer.

CD spectropolarimetry of peptide **7HSAP1a-CAP** confirmed its helical conformation with distinctive minima at 208 nm and 222 nm. The CD signals are nearly identical before or after thermal annealing of the peptides in 10mM MES buffer (pH 6.0) with or without 100 mM KF (Figure 16 and Figure 17).

Annealing influenced the behavior of **7HSAP1a** peptide much more than **7HSAP1a-CAP** peptide**,** which corresponded to the anticipation that capping of the peptide would hinder self-association. **7HSAP1a** peptide had different behavior in different buffers, which was furthered proved by TEM study.

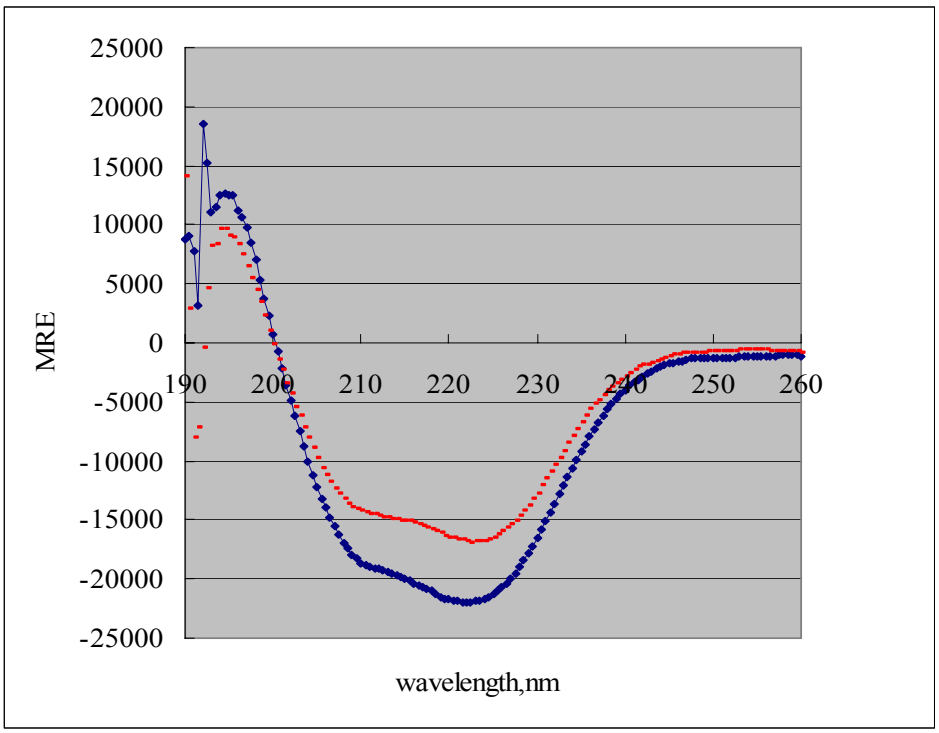

Figure 13. CD spectropolarimetry of peptide **7HSAP1a** (12.57 μM in 10 mM MES buffer pH 6.0) before (blue) and after (red) thermolysis at 95 °C and extended annealing at 25 °C.

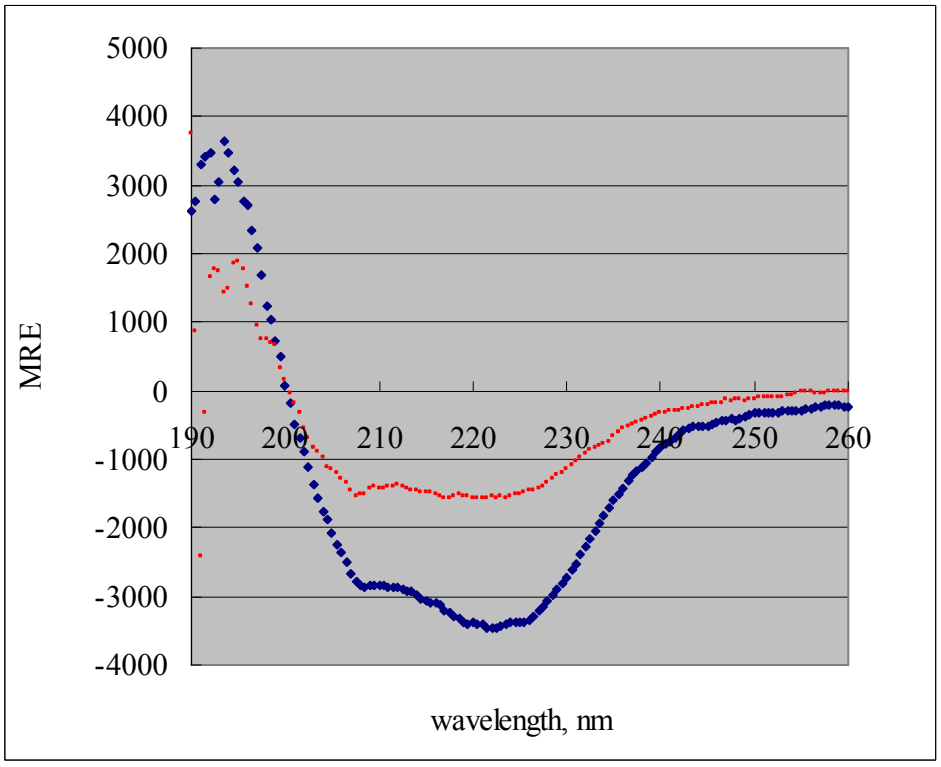

Figure 14. CD spectropolarimetry of peptide **7HSAP1a** (50.29 μM in 10 mM MES buffer pH 6.0 with 100 mM KF) before (blue) and after (red) thermolysis at 95 °C and extended annealing at 25 °C.

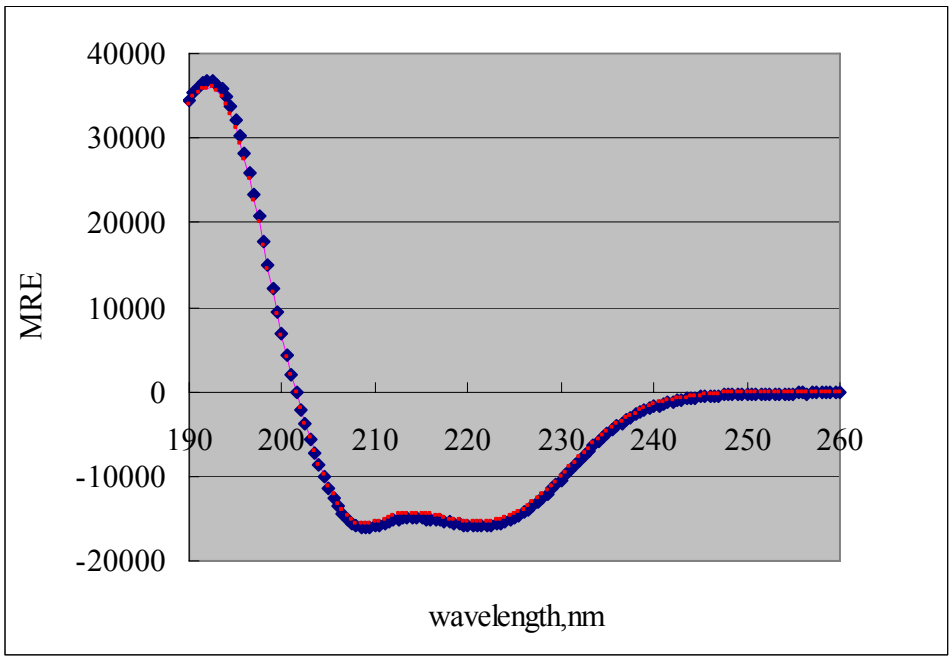

Figure 15. CD spectropolarimetry of peptide **7HSAP1a** (49.61 μM in distilled H_2O) before (blue) and after (red) thermolysis at 95 °C and extended annealing at 25 °C.

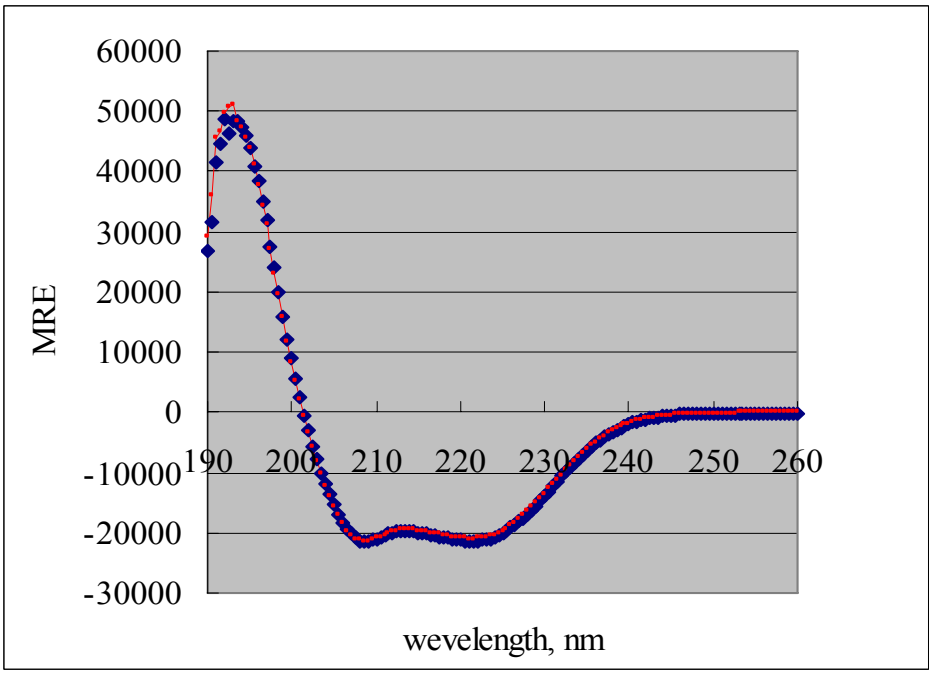

Figure 16. CD spectropolarimetry of peptide **7HSAP1a-CAP** (68.34 μM in 10 mM MES buffer pH 6.0) before (blue) and after (red) thermolysis at 95 °C and extended annealing at 25 °C.

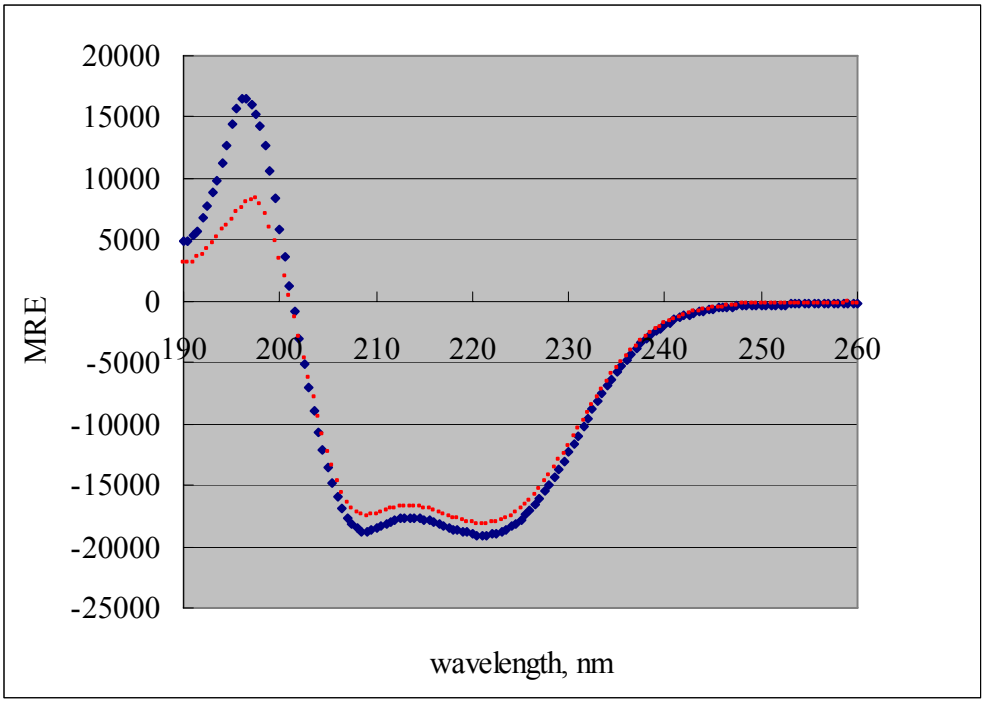

Figure 17. CD spectropolarimetry of peptide **7HSAP1a-CAP** (68.34 μM in 10 mM MES buffer pH 6.0 with 100 mM KF) before (blue) and after (red) thermolysis at 95 °C and extended annealing at 25 °C.

Transmission Electron Microscopy

TEM studies indicate the presence of high aspect-ratio fibrils of uniform diameter of 7.4nm down to a peptide concentration of 12.57 μM in 10 mM MES buffer (pH 6.0) for peptide **7HSAP1a** (Figure 18, Figure 19 and Figure 20). However, barely defined structures can be seen in the samples for peptide **7HSAP1a-CAP** in 10 mM MES buffer (pH 6.0)**.** The self-association of the capped peptide appears to be significantly inhibited with respect to the uncapped peptide when treated under identical conditions (Figure 21). In the presence of 100 mM KF in 10 mM MES buffer, well-defined structures are formed for peptide **7HSAP1a** (Figure 22) but not for peptide **7HSAP1a-CAP**. Fibril structures can be seen for peptide **7HSAP1a** in distilled H_2O (Figure 23).

Given similar concentration in different buffers, the self-assembly behavior for **7HSAP1a** peptide was enhanced in MES buffer (pH 6.0, 100 mM KF), but was weakened in distilled H_2O, corresponding to the results from CD study, which might provide a hint to a point that the self-assembly could be controlled. In the case of capped peptide **7HSAP1a-Cap**, self-assembly of fibrils was greatly inhibited after thermal annealing of peptide solutions, confirming the anticipation the capping would hinder the self-assembly behavior of the peptide.

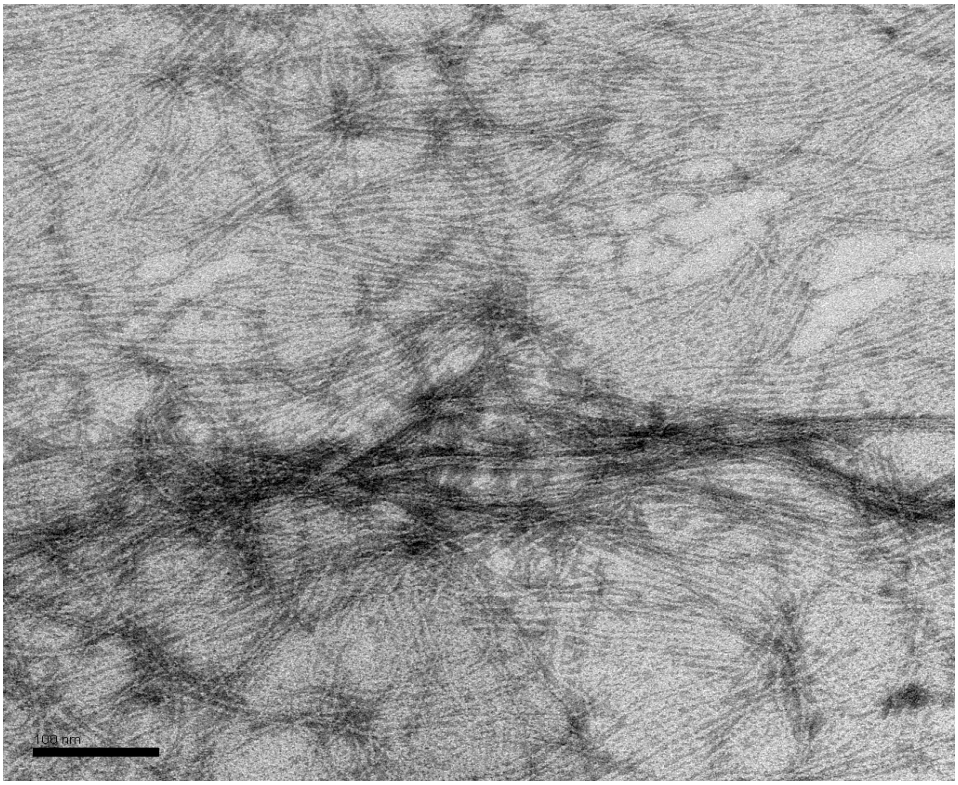

Figure 18. TEM image of high aspect-ratio fibrils that result from self-assembly of peptide **7HSAP1a** (50.29 μM in 10 mM MES buffer pH 6.0) after thermolysis at 95 °C and extended annealing at 25 °C (scale bar = 100 nm).

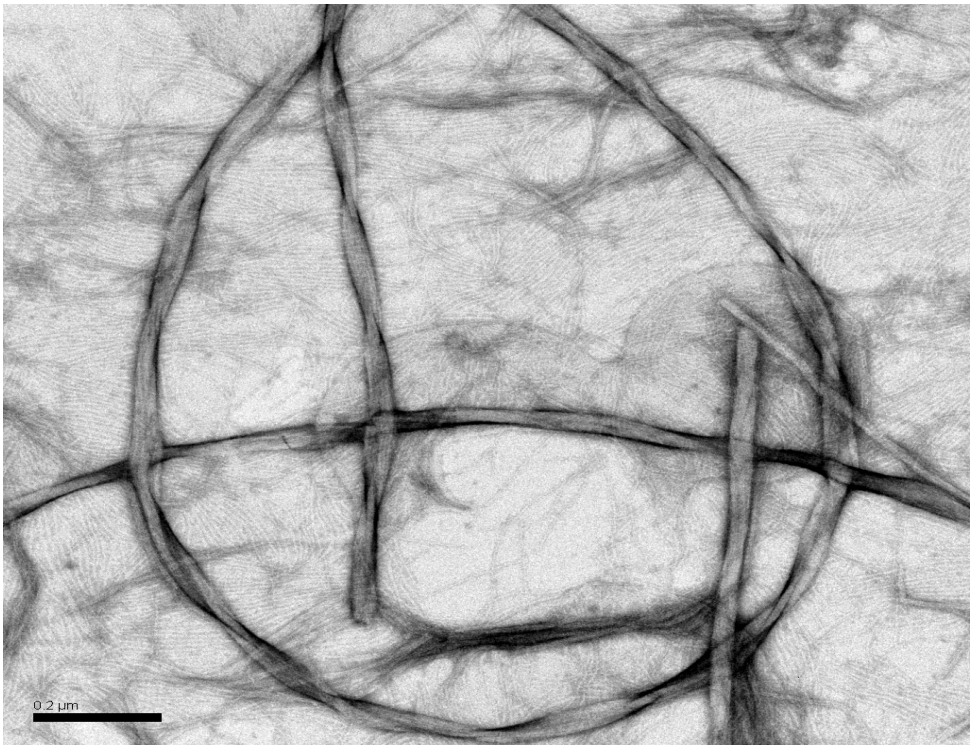

Figure 19. TEM image of high aspect-ratio fibrils that result from self-assembly of peptide **7HSAP1a** (50.29 μM in 10 mM MES buffer pH 6.0) after thermolysis at 95 °C and extended annealing at 25 °C (scale bar = 200nm).

Figure 20. TEM image of high aspect-ratio fibrils that result from self-assembly of peptide **7HSAP1a** (12.57 µM in 10 mM MES buffer pH 6.0) after thermolysis at 95 °C and extended annealing at 25 °C (scale bar = 200nm).

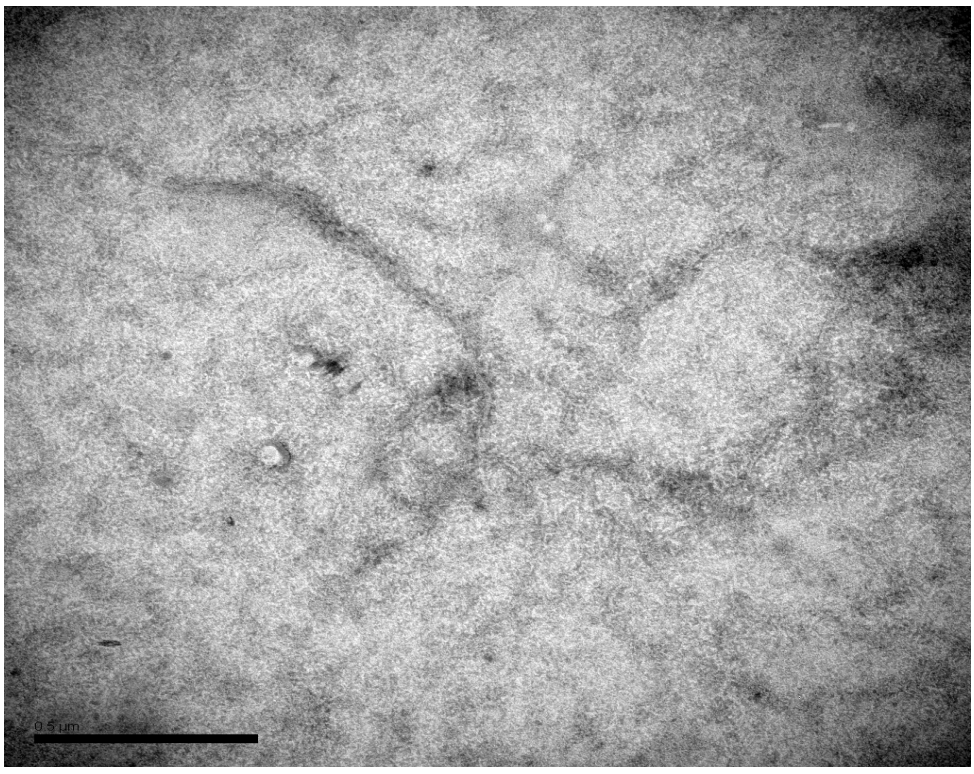

Figure 21. TEM image of peptide **7HSAP1a-CAP** (68.34 µM in 10 mM MES buffer pH 6.0) after thermolysis at 95 °C and extended annealing at 25 °C (scale bar = 500nm).

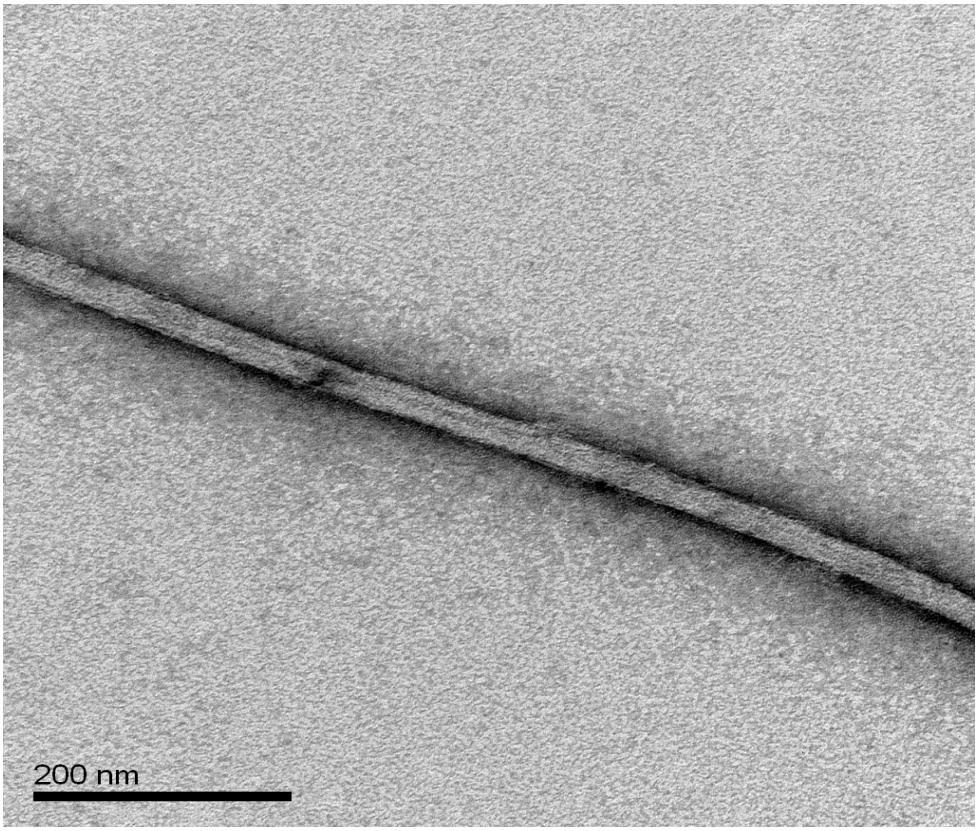

Figure 22. TEM image of peptide **7HSAP1a** (50.29 μM in 10 mM MES buffer pH 6.0 with 100 mM KF) after thermolysis at 95 °C and extended annealing at 25 °C (scale bar = 200nm)

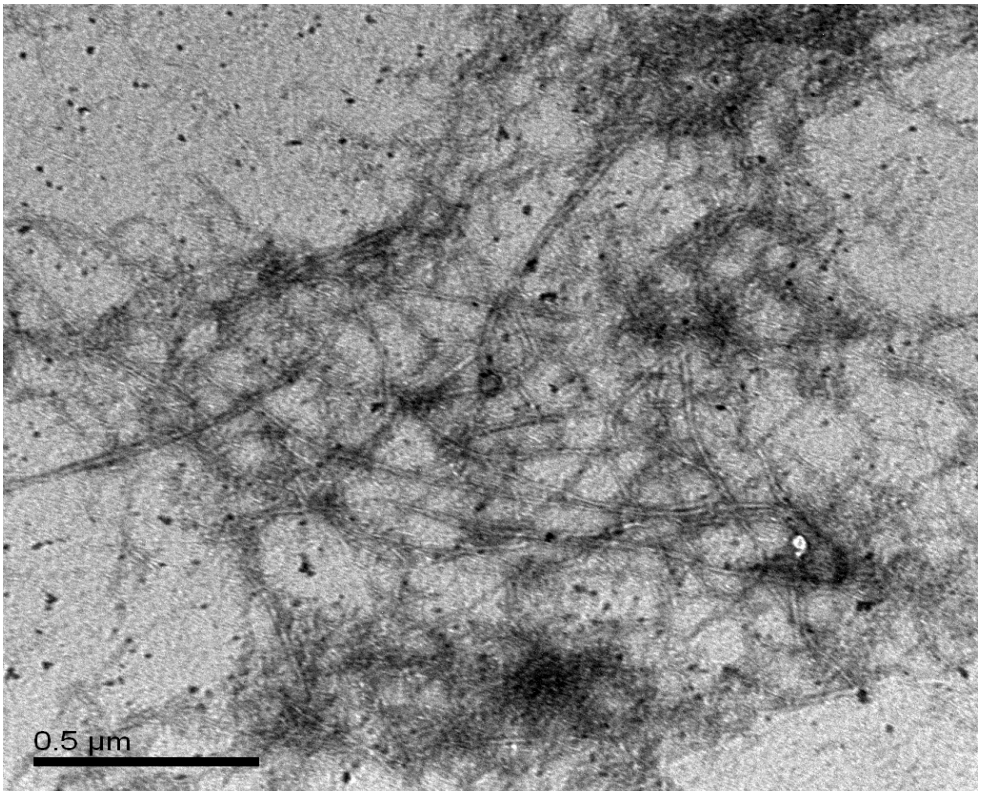

Figure 23. TEM image of peptide **7HSAP1a** (49.61 μM in distilled H_2O) thermolysis at 95 °C and extended annealing at 25 °C (scale bar = 500nm)

Fluorescence Spectroscopy

The solvatochromic fluorophore 6-propionyl-2-dimethylaminonaphthalene (PRODAN) was employed as a probe to assess the ability of the assembly to encapsulate small-molecules of appropriate size. The concentration of the standard solution of PRODAN in DMF was determined to be 588.44 μM by UV spectrophotometry. Fluorescence spectra were first investigated for the standard solution of 588.44 μM PRODAN in DMF and 2.57 μM PRODAN in 500 μL of 10 mM MES buffer (pH 6.0) as the reference lines (Figure 24). PRODAN in DMF showed a peak around 461 nm. PRODAN in 10 mM MES buffer (pH 6.0) exhibited similar spectrum of PRODAN in water with 531 nm as the maximum. This wavelength shift in fluorescent emission is consistent with the previously reported solvatochromic shifts of PRODAN solutions [18].

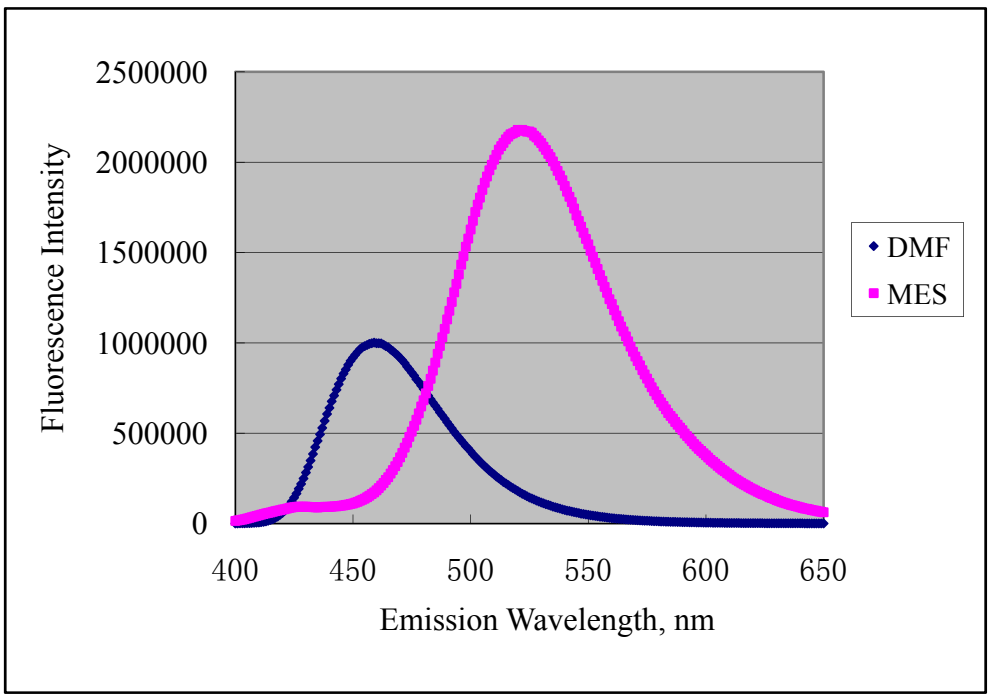

Figure 24. Fluorescence spectra for 588.44 μM PRODAN in DMF and 2.57 μM PRODAN in 10 mM MES buffer (pH 6.0)

A concentration of PRODAN was adjusted to a constant value of 2.57 μM in 500 μL of 10 mM MES buffer pH 6.0 and **7HSAP1a-CAP** peptide was added to final concentrations of 68 μM, 137 μM, 200 μM and 273 μM with or without thermal annealing (Figure 25). In terms of the peptide without annealing, two peaks of around 434 nm and 531 nm were observed. The peak for PRODAN in DMF was not observed due to the small volume of DMF in the samples. The peak around 531 nm was the peak of PRODAN in water; whereas with the increase of the concentration of the peptide, the peak around 434 nm became more and more intense, which indicated the inclusion of PRODAN to the hydrophobic cavity formed by the peptide. The increase in fluorescent emission of PRODAN as a function of the increase in peptide concentration strongly resembles the fluorescent behavior of PRODAN inclusion within γ-cyclodextrin [18]. The internal cavities should be approximately similar in diameter between the capped seven-helix bundle of 7HSAP1a-Cap and γ-cyclodextrin. A different fluorescent response was observed for inclusion of PRODAN within the smaller internal cavity of β-cyclodextrin [18]. In contrast, only a weak emission at around 434 nm was observed for peptide solutions after thermal annealing, which may be due to the formation of fibers that hinder the inclusion of PRODAN within the channel after formation.

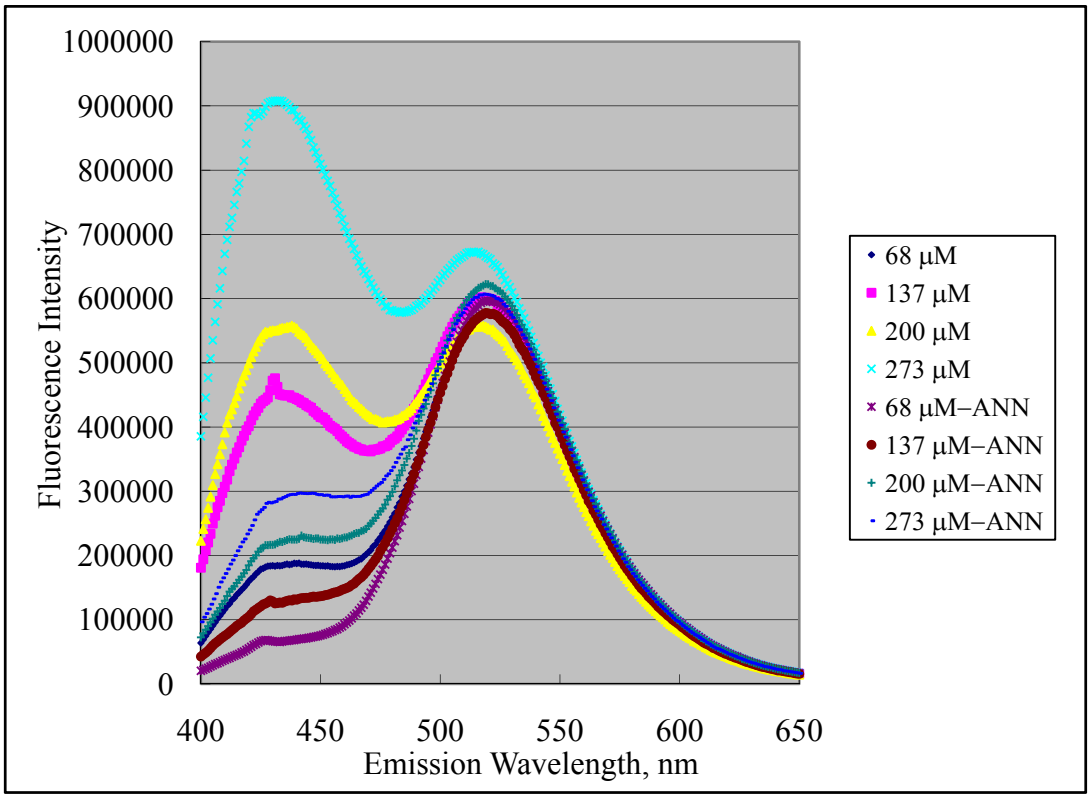

Figure 25. Fluorescence spectra for 2.57 µM PRODAN in **7HSAP1a-CAP** peptide solutions in 10 mM MES buffer (pH 6.0) at different concentrations with or without thermal annealing at 95 °C.

Fluorescence spectra were obtained for PRODAN in situ, in the presence of peptides **7HSAP1a** and **7HSAP1a-CAP** at fixed concentration of 250 µM as a function of temperature. Fluorescence emission spectra were recorded within the range from 25 °C to 75 °C in increments of 10 °C with an equilibration of 10 minutes at each temperature (Figure 26 and Figure 27). For both peptides, the emissive peak around 434 nm became weaker with the increase of the temperature. This temperature increase usually coincides with enhanced formation of fibers, which can hinder the inclusion of PRODAN and consequently result in a shift in the solvatochromic emmision. Spectra were also obtained after the temperature cooling back to 25 °C. The peak around 434 nm for the **7HSAP1a-Cap** was much higher than that of

7HSAP1a peptide, which might due to the higher capacity of **7HSAP1a** peptide to form fibers that hinder inclusion of PRODAN in comparison to the **7HSAP1a-Cap** peptide.

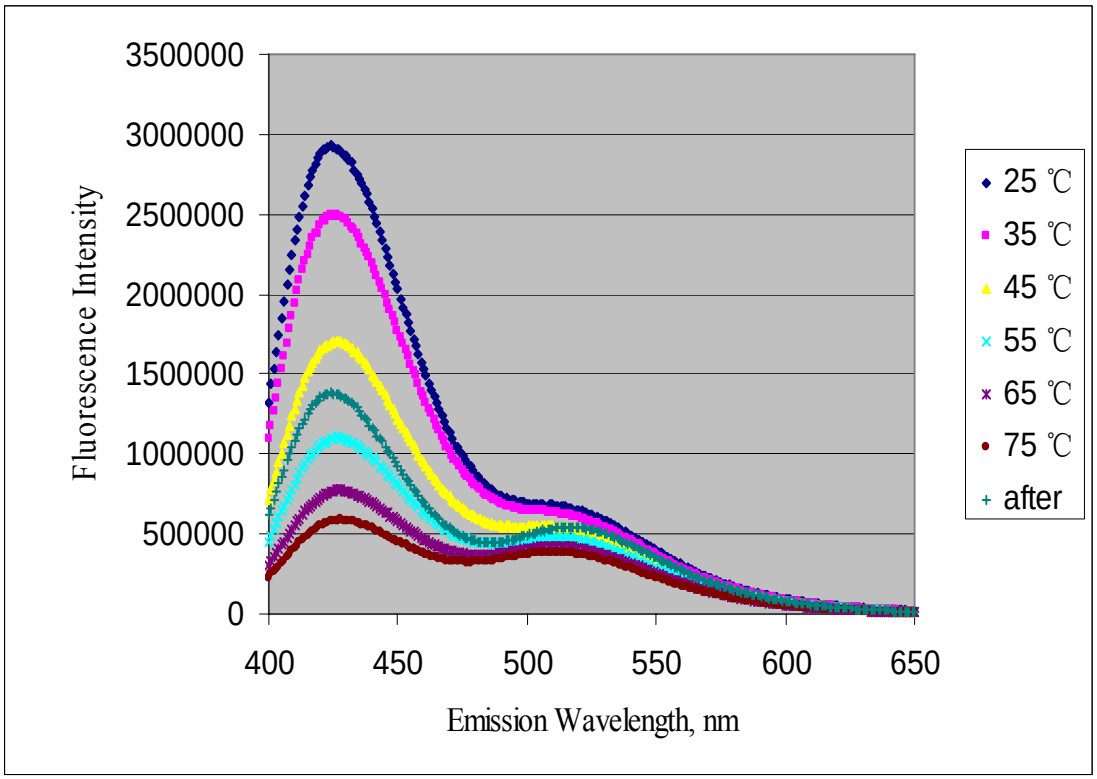

Figure 26. Fluorescence spectra for 2.57 μM PRODAN in 250 μM **7HSAP1a** peptide solutions in 10 mM MES buffer (pH 6.0) at temperature range from 25 °C to 75 °C.

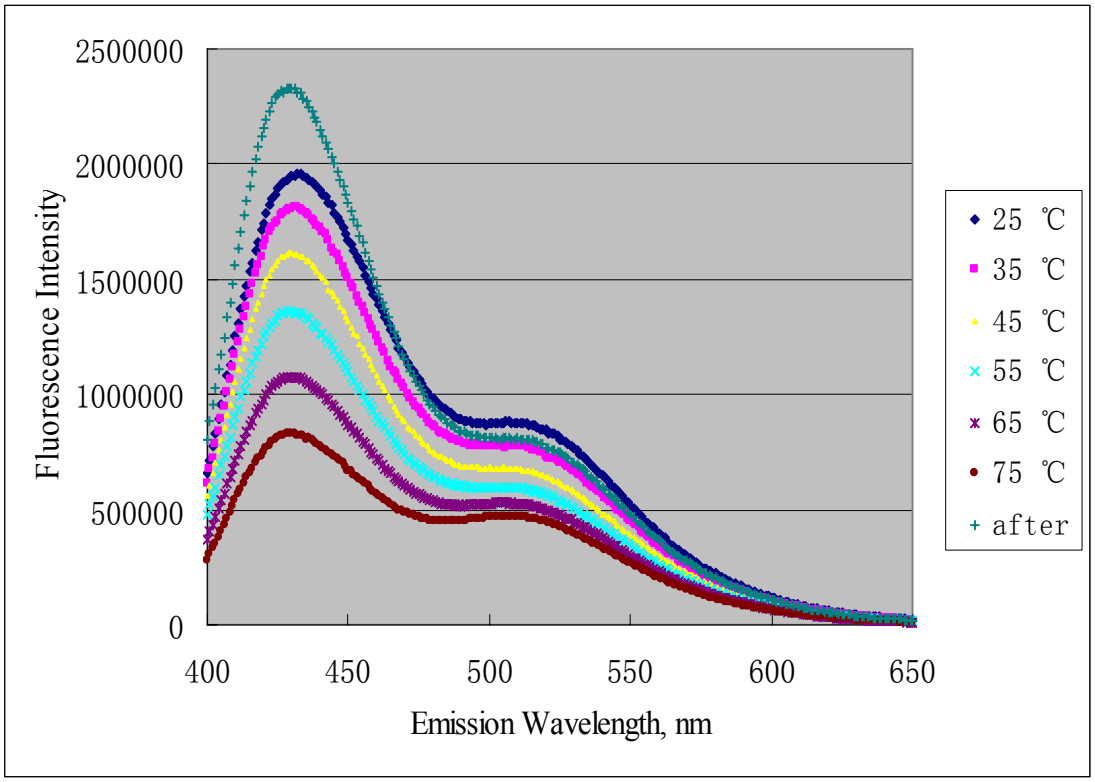

Figure 27. Fluorescence spectra for 2.57 μM PRODAN in 250 μM **7HSAP1a-Cap** peptide solutions in 10 mM MES buffer (pH 6.0) at temperature range from 25 °C to 75 °C.

Conclusion:

The goal of the project is to promote the formation of an extended helical fibril from self-assembly of seven-helix bundle and to investigate the formation of coiled-coil channel by the peptides. The peptide，**7HSAP1a,** maintained an α–helical secondary structure and formed high aspect-ratio fibrils of uniform diameter of 7.4 nm. By modifying the sequence of the peptide that created a discrete seven-helix bundle, association between the ends of the lock washer structures was promoted, which resulted in self-assembly to a helical fibril structure from dilute solutions of peptide in MES buffer. The **7HSAP1a-CAP** peptide was investigated as a negative control, which confirmed that the uncapped ends were necessary to promote electrostatic attraction between the lock washer structures at the interface between the ends of the helices, and thus facilitate self-assembly into extended helical structures. Fluorescence spectroscopy study confirmed the anticipation that the **7HSAP1a** peptide might form a coiled-coil channel that was capable of trapping small-molecule probes such as the solvatochromic fluorophore PRODAN. However, conditions that favored fiber formation seemed to reduce the capacity of the assembly to bind PRODAN, which suggests that PRODAN might be too large to permit fiber assembly when encapsulated within an inclusion complex. In analogy to cyclodextrin chemistry, smaller guest molecules might be included within the assembly as quasi-stable species as long as they do not hinder self-association of the lock washer units into extended fibers. We anticipate that if peptide nanotubes of appropriate dimension could be designed and synthesized that could encapsulate small-molecules of pharmaceutical

interest within a self-assembled material.

References:

[1] Woolfson, D.N. Building fibrous biomaterials from α-helical and collagen-like coiled-coil peptides. *Biopolymers*, **2010**, 94: 118–27.

[2] Wolf, E.; Kim, P.S.; Berger, B. A guided tour in protein interaction space: coiled coils from the yeast proteome. *Protein Sci.* **1997**, 6, 1179-89.

[3] Mason, J.M.; Arndt, K.M. Coiled-coil domains: stability, specificity, and biological implications. *ChemBioChem*, **2004,** 5, 170-6.

[4] Crick, F.H.C. The packing of α-helices: simple coiled-coils. *Acta Crystallogr*, **1953**, 6, 689-97.

[5] Diao, J.Sh. Crystal structure of a super leucine zipper, an extended two-stranded super long coiled coil. *Protein Science*, **2010**, 19, 319-26.

[6] O'Shea E.K.; Klemm J.D.; Kim P.S.; Alber, T. X-ray structure of the GCN4 leucine zipper, a two-stranded, parallel coiled coil. *Science,* **1991**, 254, 539–44.

[7] Grigoryan, G.; Keating, A.E. Structural specificity in coiled-coil interactions. *Curr. Opin. Struct. Biol.* **2008**, 18, 477-83.

[8] Tang, Y.; Tirrell, D.A. Biosynthesis of a highly stable coiled-coil protein containing hexafluoroleucine in an engineered bacterial host. *J.Am.Chem.Soc.* **2001**, 123, 11089-90.

[9] Potekhin, K.J.; Medvedkin, V.N.; Kashparov, I.A.; Venyaminov, S. Buried asparagines determine the dimerization specificities of leucine zipper mutants. *Protein Eng.* **1994**, 7, 1097-101.

[10]Liu, J.; Zheng, Q; Deng, Y.Q. Kallenback, N.R.; Lu, M. Conformational transition between four and five- stranded phenylalanine zippers determined by a local packing interaction. *J Mol Biol*, **2006**, 361, 168-79.

[11]Zhou, N.E.; Kay, C.M.; Hodges, R.S. Protein destabilization by electrostatic repulsions in the two-stranded alpha-helical coiled-coil/leucine zipper. *Protein Sci.* **1995**, 4, 237-50.

[12]Zeng, X.; Zhu, H.; Lashuel, H.A.; Hu, J. C. Oligomerization properties of GCN4 leucine zipper *e* and *g* position mutants. *Protein Sci.* **1997**, 6, 2218-26.

[13]Koronakis, V.; Sharff, A.; Koronakis, E.; Luisi, B.; Hughes, C. Crystal structure of the bacterial membrane protein TolC central to multidrug efflux and protein export. *Nature*, **2000**, *405*, 914-9.

[14]Liu, J.; Zheng, Q.; Deng, Y.; Cheng, C.S.; Kallenbach, N.R.; Lu, M. A seven-helix coiled coil. *Proc. Natl. Acad. Sci. USA,* **2006**, *103*, 15457-62.

[15]Sabatino, G.; Chelli, M.; Brandi, A.; Papini, A. M. Analytical methods for solid phase peptide synthesis. *Current Organic Chemistry*, **2004**, *8,* 291-301.

[16]Carpino, L.A.; Han, G. Y. 9-Fluorenylmethoxycarbonyl amino-protecting group. *J. Org. Chem.*, **1972**, *37*, 3404–9.

[17]Nilsson, B.L.; Soellner, M.B.; Raines, R.T. Chemical synthesis of proteins. *Annu.Rev. Biophys. Biomol. Struct.* **2005**, 34, 91–118.

[18]Crane, N.J.; Mayrhofer, R. C.; Betts, T. A. Cyclodextrin inclusion complexes with a solvatochromic fluorescent probe. *JChemEd*, **2002**, 79, 1261-3.